Thickness dependence of the structural and electrical properties of ZnO thermal-evaporated thin films

A GHADERI[1,*], S M ELAHI[2], S SOLAYMANI[3], M NASERI[4], M AHMADIRAD[5], S BAHRAMI[1] and A E KHALILI[1]

[1]Department of Physics, Islamic Azad University-Tehran Central Branch, Tehran, Iran
[2]Plasma Physics Research Center, Science and Research Branch, Islamic Azad University, Tehran, Iran
[3]Young Researchers Club, Kermanshah Branch, Islamic Azad University, Kermanshah, Iran
[4]Department of Physics, Islamic Azad University, Kermanshah Branch, Kermanshah, Iran
[5]Institute for Research of Fundamental Science (IPM), Tehran, Iran
*Corresponding author. E-mail: atefeh.ghaderi@gmail.com

Abstract. ZnO thin films of different thicknesses were prepared by thermal evaporation on glass substrates at room temperature. Deposition process was carried out in a vapour pressure of about 5.54×10^{-5} mbar. The substrate–target distance was kept constant during the process. By XRD and AFM techniques the microstructural characteristics and their changes with variation in thickness were studied. Electrical resistivity and conductivity of samples vs. temperature were investigated by four-probe method. It was shown that an increase in thickness causes a decrease in activation energy.

Keywords. Zinc oxide thin film; thermal evaporation; X-ray diffraction; atomic force microscope; electrical conductivity.

PACS No. 73

1. Introduction

Zinc oxide is an n-type semiconductor with hexagonal wurtzite structure. Some recent works have reported the preparation of p-type ZnO films obtained by suitable doping [1–3]. It has attracted much attention as transparent conducting oxide (TCO) films, as electrodes in solar cells [4,5], as gas sensors [6], in nanolaser and other photoluminescent devices [7,8] and more recently as thin film transistors [9].

ZnO can be used in different forms, like single crystals, sintered pellets and thin films. Thin films have exhibited a wide variety of applications in environmental engineering, catalysis and gas sensor systems because they can be fabricated in small dimensions, in large scale and low cost and are widely compatible with microelectronics technology [10].

Several techniques were used to synthesize ZnO thin films, namely, sputtering [11,12], spray pyrolysis [13], sol–gel [14] and evaporation [15].

However, the evaporation method is perhaps the cleanest and relatively simple and it is a low-cost technique that can be used to prepare low-melting point, low-decomposition, or low-sublimation point oxides [16]. In this method parameters are easily controllable, and consequently, thin films with different structures and properties can be obtained by changing the preparation parameters. Thus, in the present work, we have paid much attention in preparing thin films of ZnO on glass substrate by thermal evaporation technique.

2. Experimental procedure

The ZnO thin films were prepared by the thermal evaporation of Zn granules (Merck) of high purity (99.999%) placed on a molybdenum boat. Glass substrates were used and substrate–target distance was kept constant. The system was pumped in an evaporating chamber to a final vapour pressure of about 5.54×10^{-5} mbar and then heated by Joule effect. To study the influence of thickness, deposition was carried out in different thicknesses by changing the evaporation time. The thickness of the films was measured by Tencor Alpha-step 500 profiler. The thicknesses of ZnO thin films are shown in table 1. To determine the crystalline structure, X-ray diffraction (XRD) was used. Atomic force microscope (AFM) was used to study the surface topography of the ZnO films.

To study the electrical properties, gold contacts were deposited on the surface of the samples by evaporation method. Electrical measurements in different thicknesses were carried out by four-probe method. The *I–V* characteristics of the thin films were measured with a programmable voltage source which scans the DC voltage at a speed of 1 V/min. By this method, the resistance, resistivity, conductivity and activation energy were obtained in different temperatures. Changes in the semiconductive property of ZnO thin films were evaluated by these parameters.

3. Results and discussion

3.1 *XRD studies*

Figure 1 shows three typical XRD patterns of the investigated samples in three different thicknesses. As one can see from figure 1a, the sample S1 has monocrystalline structure with orientation along (1 0 0) axis but the intensity of this peak in relation to the other samples, as can be seen in table 1, can be neglected. It is worth to mention that the glass

Table 1. Film thickness parameters for samples S1, S2 and S3.

Sample	Deposition time (s)	Film thickness (nm)
S1	20	30
S2	40	60
S3	60	75
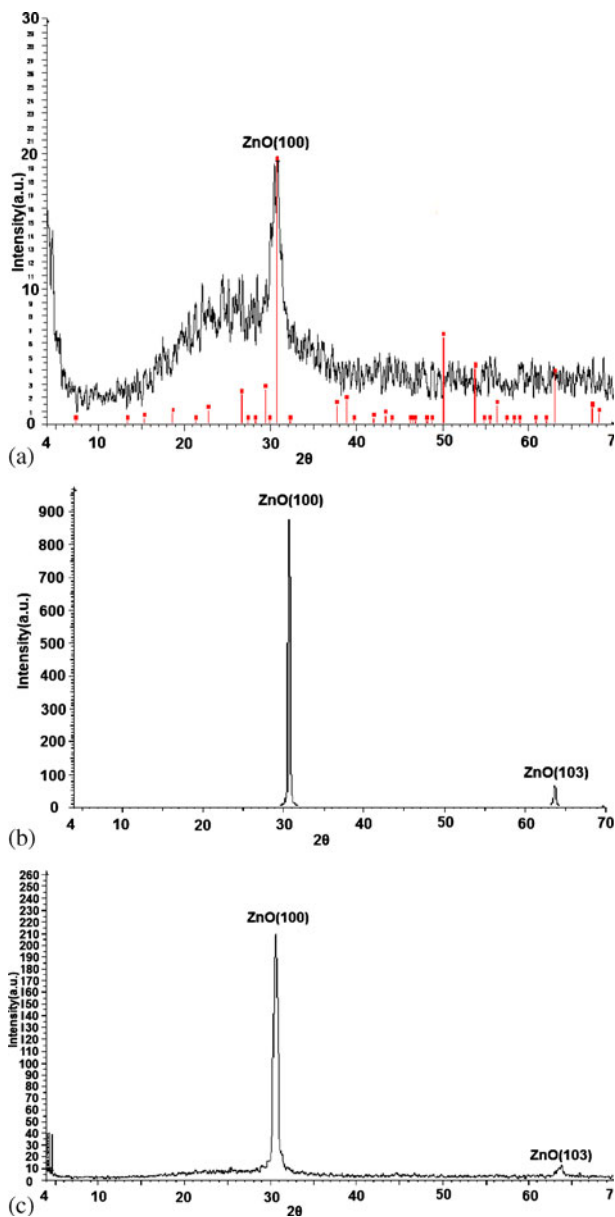
Figure 1. XRD patterns for normally evaporated ZnO films: (**a**) S1, (**b**) S2, (**c**) S3.

amorphous structure, that is clear in the baseline of the curve indicates the low thickness of the sample S1. Figures 1b and c show the polycrystalline structure. These samples exhibit the same preferential orientation along (1 0 0) and (1 0 3) axes respectively in $2\theta = 31°$ and $64°$ of the ZnO hexagonal wurtzite structure [17]. ZnO peak intensity of the samples can be compared in table 2.

Table 2. Intensity in each axis of the samples.

Sample	I_{hkl}	
	(1 0 0)	(1 0 3)
S1	19	–
S2	850	60
S3	200	15

X-ray diffraction (XRD) was used to determine crystalline structure and size of the particles. The ZnO crystallite sizes are calculated from the following Debye–Scherrer formula:

$$D = \frac{0.89\lambda}{\beta_{hkl} \cos\theta}.$$ (1)

In this formula $\lambda = 15.418$ nm is the wavelength of CuK_α radiation in the 2θ confine (from $20°$ to $80°$) and θ, the Bragg's angle, in all samples for ZnO peak along (1 0 0) orientation is $31°/2$ and β_{hkl} is the broadening of the full-width at half-maximum (FWHM). These results are shown in table 3.

3.2 *AFM studies*

Figure 2 presents a selection of 1 μm $\times$ 1 μm sized atomic force micrographs of the investigated ZnO thin films of various thicknesses. In sample with the lowest thickness, particles rather are isolated from each other (figure 2a) while in figures 2b and c these are continually in distribution. This suggests that the particles seen at the surface of the film are clusters of crystallites.

Figure 2d estimates the surface topography by the size of the particles and their abundance. The Gaussian charts for all the samples indicate that distribution of particles is nearly monotonous. The width of the peak for the sample S3 is more than other samples. It means that the size of nanoparticles is more distributed in S3. Moreover, surface roughness and particles abundance are low. The sharpness of peaks in S2 and S1 shows that their surface is smoother than S3.

The size of the nanoparticles which was approximated by Debye–Scherrer formula (1) and due to the AFM images (figure 2 and table 3) are approximately in the same ordered magnitudes. That is, XRD and AFM results agree with each other.

Table 3. Size of particles estimated by Debye–Scherrer formula and AFM images.

Sample	D (nm) XRD	D (nm) AFM
S1	10.97	10
S2	30.18	22
S3	16.09	14

(a)　　　　　　　　　(b)　　　　　　　　　(c)

(d)
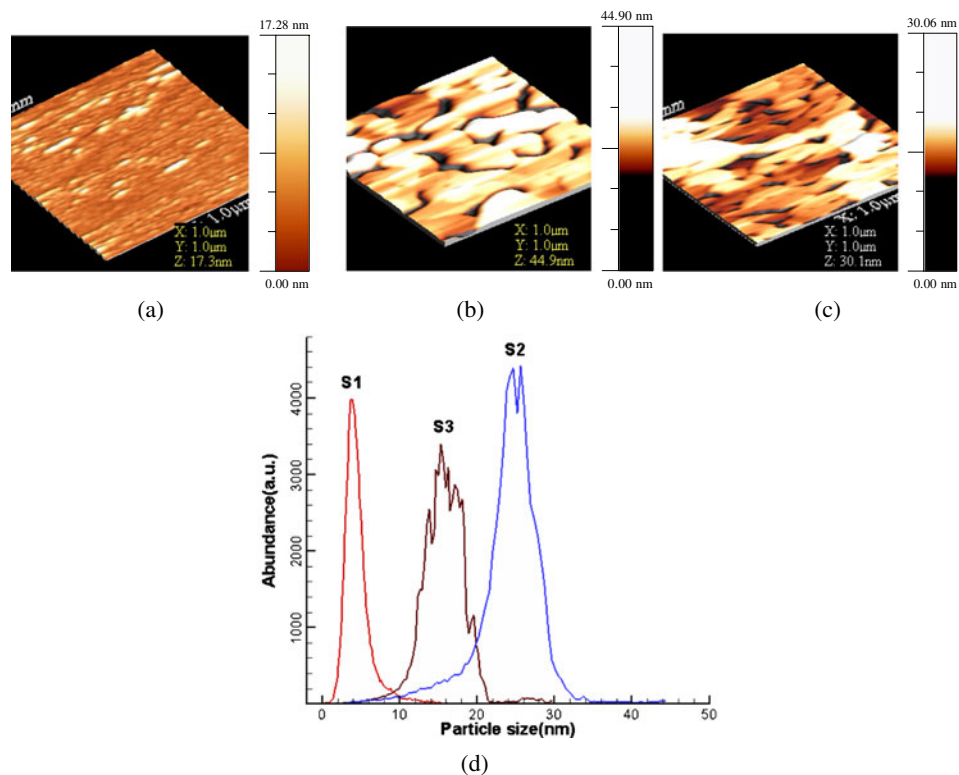
Figure 2. AFM picture of the as-prepared samples with their topography **(a)** S1, **(b)** S2, **(c)** S3, **(d)** abundance vs. particle size (nm).

3.3 *Electrical studies*

As shown in figure 1a and table 2, the intensity of the peak for sample S1 at (1 0 0) orientation is too weak and it can be deduced that the thin film's thickness is less. Therefore, the conductivity is negligible. This result was confirmed by the electrical measurements. The $I-V$ characteristic curves of S2 and S3 samples in different temperatures (35°C–75°C) are shown in figure 3.

The electrical resistance (Ω) of the S2 and S3 samples can be obtained from the $I-V$ curves by calculating the gradients of the curves. So, resistivity (Ω-cm) can be computed at each temperature. Gradient of curves in S3 is more than S2, i.e. when thickness increases even the gradient increases. It emphasizes fall of resistance.

The resistivity of each sample was calculated using eq. (2) [18].

$$\rho = \frac{\pi t}{\ln 2}\left(\frac{V}{I}\right), \tag{2}$$

where ρ is the resistivity (Ω-cm), t is the sample thickness (cm), V is the measured voltage and I is the source current (A).

Figure 4 shows the dependence of resistivity on temperature.
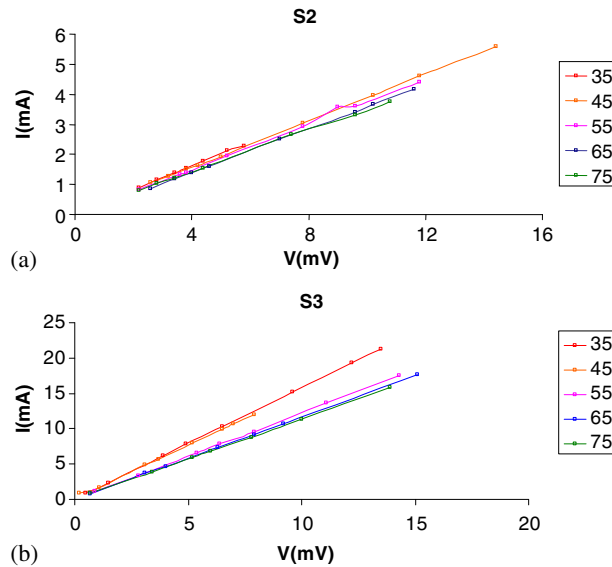
Figure 3. Variations of current vs. voltage by increasing the temperature for **(a)** S2, **(b)** S3.

It is clear that when temperature increases the resistivity decreases, which indicates a semiconductive property [19]. In comparison samples, at fixed temperature, by increasing the thickness the resistivity decreases. It is useful, in discussions on variations of resistivity, to examine the behaviour of conductivity. According to eq. (3), by plotting $\ln(\sigma)$ vs. $1/T$, the activation energy can be found.

$$\sigma = \sigma_0 e^{-E/kT}, \tag{3}$$

where σ is the conductivity $(1/\rho)$, E is the activation energy (eV), k is the Boltzmann constant and T is the temperature (K).

The calculated activation energies are:

$$E(S2) = 7.45 \times 10^{-26} \text{ eV}$$

$$E(S3) = 5.52 \times 10^{-26} \text{ eV}$$

From the calculations and figure 5 it can be seen that when the thickness increases, activation energy decreases. In fact, the electrical activation energy is equal to the energy
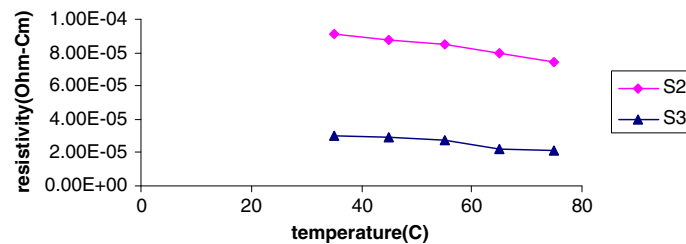
Figure 4. Decrease in resistivity by increasing the temperature and thickness.
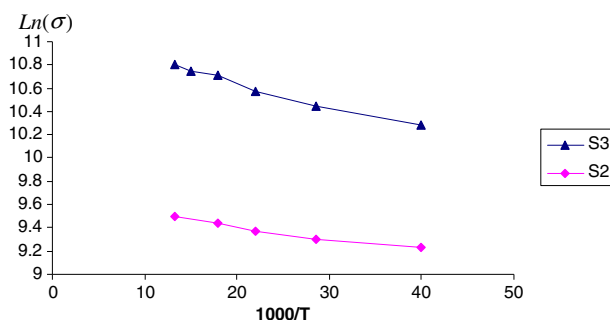
Figure 5. Conductivity vs. inversion of temperature for different thicknesses.

difference between Fermi level and the bottom of the conduction band. Hence, the activation energy can be used as a tool for determining Fermi level position [15].

4. Conclusions

In this research ZnO thin films of different thicknesses were prepared by thermal evaporation on glass substrates. The preferred orientations in the samples were in (1 0 0) and (1 0 3) axes respectively in $2\theta = 31°$ and $64°$ of ZnO hexagonal wurtzite structure.

Electrical properties of the samples were studied by four-probe method. It can be seen from figures 3–5 that there is a decrease in resistance and resistivity, an increase in conductivity and finally a decrease in activation energy by increasing the thickness in the same temperature range.

The decrease in the activation energy due to the increase in thickness indicates clearly that the semiconducting property is increasing with increase in thickness.

References

[1] Y R Ryu, S Zhu, D C Look, J M Wrobel, H M Jeong and H W White, *J. Crystal Growth* **216(1–4)**, 330 (2000)
[2] C Wang, Z Ji, J Xi, J Du and Z Ye, *Mater. Lett.* **60(7)**, 912 (2006)
[3] X L Guo, H Tabata and T Kawai, *J. Crystal Growth* Part I **237–239**, 544 (2002)
[4] S Fay, S Dubali, U Kroll, J Meier, Y Zeigler and A Shah, in: *Proceedings of the 16th Photovoltaic Solar Energy Conference*, 2000, p. 362
[5] J Muller, O Kulth, S Wieder, H Siekmann, G Schope, W Reetz, O Vetterl, D Lundzien, A Lambertz, F Finger, B Rech and H Wagner, *Solar Energy Mater. Solar Cells* **66**, 275 (2001)
[6] H Nanto, T Minami and S Takata, *J. Appl. Phys.* **60**, 482 (1986)
[7] D M Bagnall, Y F Chen, Z Zhu, T Yao, S Koyama, M Y Shen and T Gato, *Appl. Phys. Lett.* **70**, 2230 (1997)
[8] M A Hasse, J Qui, J M De Puydt and H Cheng, *Appl. Phys. Lett.* **59**, 1272 (1991)
[9] E Fortunato, P Barquinha, A Pimentel, A Goncalves, A Marques, L Pereira and R Martins, *Thin Solid Films* **487**, 205 (2005)
[10] M Suchea, S Christoulakis, M Katharakis, G Kiriakidis, N Katsarakis and E Koudoumas, *Appl. Surf. Sci.* **253**, 8141 (2007)

[11] P Nunes, D Costa, E Fortunato and R Martins, *Vacuum* **64**, 293 (2002)

[12] K H Kim, K C Park and D Y Ma, *J. Appl. Phys*. **81**, 7764 (1997)

[13] P M Ratheesh Kumar, C Sudha Kartha, K P Vijayakumar, F Singh and D K Avasthi, *Mater. Sci. Eng.* **B117**, 307 (2005)

[14] A Abdel Aal, S A Mahmoud and A K Aboul-Gheit, *Nanoscale Res. Lett.* **4**, 627 (2009), DOI: 10.1007/s11671-009-9290-1

[15] N Bouhssire, S Abed, E Tomasella, J Cellier, A Mosbah, M S Aida and M Jacquet, *Appl. Surf. Sci.* **252**, 5594 (2006)

[16] S Panda, N Singh, J Hooda and C Jacoba, *Cryst. Res. Technol*. **43**, 751 (2008)

[17] G G Rusu, M Rusu and N Apetroaei, *Thin Solid Films* **515**, 8699 (2007)

[18] Four- Point Probe Manual, EECS143, Microfabrication Technology

[19] M Suchea, S Christoulakis, M Katharakis, N Vidakis and E Koudoumas, *Thin Solid Films* **517**, 4303 (2009)